THE JOURNAL OF PHYSICAL CHEMISTRY C

Article

pubs.acs.org/JPCC

Charge Transfer and Exciplex Emissions from a Naphthalenediimide-Entangled Coordination Framework Accommodating Various Aromatic Guests

Virginia Martínez-Martínez,*[,†] Shuhei Furukawa,[‡,§] Yohei Takashima,[§,∥] Iñigo López Arbeloa,[†] and Susumu Kitagawa[‡,§,∥]

[†]Departamento de Química Física, Universidad del País Vasco, (UPV-EHU), Apartado 644, 48080-Bilbao, Spain

[‡]Institute for Integrated Cell-Material Sciences (WPI-iCeMS), Kyoto University, Yoshida, Sakyo-ku, Kyoto 606-8501, Japan

[§]ERATO Kitagawa Integrate d Pores Project, Japan Science and Technology Agency (JST), Kyoto Research Park, Building 3, Shimogyo-ku, Kyoto 600-8815, Japan

[∥]Department of Synthetic Chemistry and Biological Chemistry, Graduate School of Engineering, Kyoto University, Katsura, Nishikyo-ku, Kyoto 615-8510, Japan

S *Supporting Information*

ABSTRACT: A detailed photophysical study was performed on an entangled porous coordination polymer (PCP) containing *N*,*N*′-dipyrid-4-yl-1,4,5,8-naphthalenediimide (dpNDI) as an electron acceptor moiety and different substituted benzene guests as electron donor units by time-resolved fluorescence spectroscopy. Emission from exciplex $(A-D)^*_{EX}$ and charge transfer complex $(A^{\delta-}-D^{\delta+})^*_{CT}$ states was identified thanks to the different conformations adopted by aromatic guests in the different adsorption sites of the PCP (denominated pore A and pore B). Fluorescence lifetime values of exciplexes and charge transfer complexes linearly correlate with the dipole moments and the ionization potentials of different substituted benzene guests, respectively. We have also identified other emissive species with much lower emission efficiency, that is, emission from the NDI pillar itself and from its interaction with the benzenedicarboxylate linker.

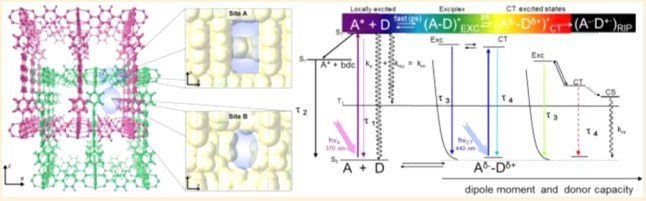

INTRODUCTION

Porous coordination polymers (PCPs) or metal−organic frameworks (MOFs), constructed by self-assembly of metal ions and organic ligands,[1−4] are special systems due to the wide variety of applications such as adsorption,[5] separation,[6] catalysis,[7] and chemical sensing.[8] Particularly, owing to the attractive characteristics of PCPs, such as designability, highly crystalline nature, intrinsic porosity, and cooperative response, they are unique systems for fine-tuning of luminescent properties.[9,10] In this sense, interesting photoactive species can be included as parts of the framework, which are arranged in a regular manner and do not aggregate, preventing fluorescence self-quenching. The nanopores allow the accommodation of a variety of guest molecules interacting with the luminescent organic scaffold in the confinement space. Moreover, in interpenetrated structures, the displacement of one framework into the other, triggered by the adsorption of molecules, will maximize host−guest interactions.

Recently, we reported a novel entangled PCP with induced-fit structural transformation, which shows an interesting guest-dependent luminescent response.[11] The PCP $[Zn_2(bdc)_2(dpNDI)]_n$ consists of 1,4- benzenedicarboxylate (bdc) acting as a layer ligand linking the dimetal Zn cluster into two-dimensional (2D) square lattices and *N*,*N*′-dipyrid-4-yl-1,4,5,8-naphthalenediimide (dpNDI) as a fluorophore pillar ligand connecting 2D lattices at the lattice points. Self-catenation of the frameworks leads to an entangled PCP with higher thermal stability than nonentangled PCPs and provides multimodal pores important for the interaction with the respective guest molecules. NDI derivatives (1,4,5,8-naphthalenediimides) are generally characterized by having low fluorescence intensity ($\Phi_{fl} \approx 0.003$) and short fluorescence lifetimes (5−18 ps).[12,13] However, because of the relatively high electron acceptor capability of NDI molecules,[14−17] they frequently show a broad red-shifted emission band with higher fluorescence intensity ($\Phi_{fl} \approx 0.02$),[12] ascribed to charge transfer (CT) complexes with aromatic hydrocarbon molecules in solution.

In this PCP, the adsorption of aromatic molecules (substituted benzenes) modifies the structure of the interpenetrated frameworks (Scheme 1, top) to maximize the CT interaction with the photoactive NDI ligand.[11] Thus, incorporating benzene derivatives with different electron-donating capacity into the pores resulted in the production of

Received: October 3, 2012
Revised: November 15, 2012
Published: November 20, 2012

   dx.doi.org/10.1021/jp309784y | *J. Phys. Chem. C* 2012, 116, 26084−26090

Scheme 1. (Top) Illustrative Representation of Framework Displacement after Aromatic Molecule Uptake and (Bottom) Geometry of the Different Pores Denominated Site A and Site B

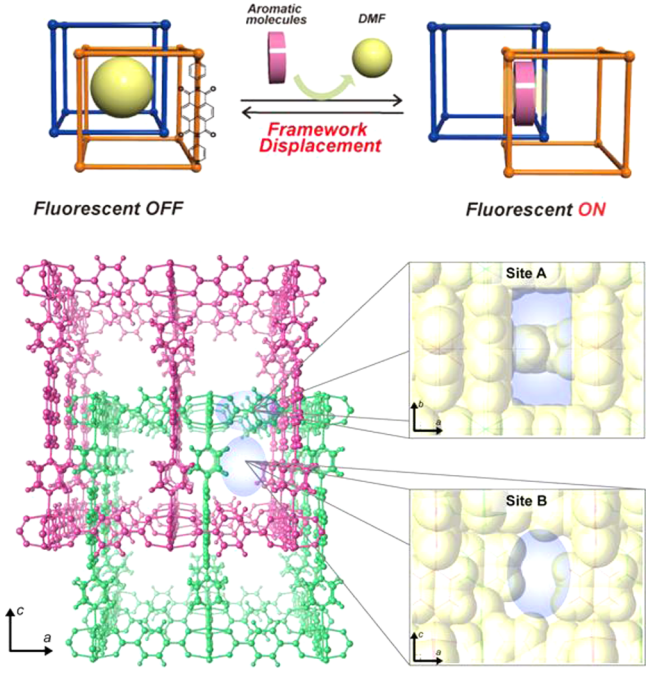

different emission colors in the whole range of the visible region (rainbow colors), apparent to the naked eye, due to the increase of the fluorescence quantum yield (Φ_{fl}) in comparison to those of complexes in solution.[11,12]

In this work, we exploit the unique structural features of this singular PCP to elucidate fine points of the CT chemistry. Particularly, it brings the possibility of discerning the photoexcited exciplex $(A-D)^*_{EX}$ and CT complex $(A^{\delta-}-D^{\delta+})^*_{CT}$ species by the confinement of aromatic guests into two different geometrically defined pores (Scheme 1, bottom). Indeed, many attempts have been made to distinguish the emission of the CT complex from the exciplex in solution. The complexity is that although the CT complex $(A^{\delta-}-D^{\delta+})^*_{CT}$ is favored in more polar solvents and the exciplex $(A-D)^*_{EX}$ in apolar solvents,[18−26] their formation is also governed by the geometric dispositions between A and D molecules, and the control of the relative A−D conformation/orientation in solution is a difficult task. In this sense, many authors have studied intramolecular emissions in several compounds with donor−acceptor moieties linked by rigid or flexible spacers with diverse lengths where the relative D−A distance and orientation are modulated by playing with the polarity of the solvent.[27−30] In those studies, so-called, compact charge transfer (CCT) species have been characterized in apolar solvents where D−A moieties are in sandwich-like geometry, similar to a tight exciplex. Conversely, the emission involves a rather large D−A separation in solvents of intermediate and high polarity with a conformation denoted as extended charge transfer (ECT).

Other attempts to explore the existence of exciplexes and excited charge transfer complexes have been made by the physical confinement of D and A in rigid systems such as fullerenes[31] and rotaxanes[32] or by the different reactivities found by choosing the excitation wavelengths in photoreactions,[33] i.e., by excitation at the CT absorption band of the complex in the ground state $(A^{\delta-}-D^{\delta+})_{CT}$ (eq 1) and/or by photoexcitation of the acceptor A* (or donor D*), which yields the exciplex $(D-A)^*_{EX}$ (eq 2).

$$A + D \rightleftarrows (A^{\delta-}-D^{\delta+})_{CT} \xrightarrow[h\nu_1]{} (A^{\delta-}-D^{\delta+})^*_{CT} \quad (1)$$

$$A + D \xrightarrow[h\nu_2]{} A^* + D \rightleftarrows (D-A)^*_{EX} \quad (2)$$

In the present work, thanks to the particular construction of this entangled PCP with two well-defined adsorption sites (Scheme 1, bottom) (site A, a slit type pore, in which the aromatic guest molecules interact in a face-to-face manner with the NDI ligand, and site B, an undulated one-dimensional channel, where aromatic guest molecules are not so structurally restricted), different emissions from both the exciplex and charge transfer complex states are characterized by steady-state and time-resolved fluorescence spectroscopy.

EXPERIMENTAL DETAILS

UV−vis diffuse reflectance measurements were recorded on a JASCO V-670 spectrometer with an integration sphere attachment. Powdered samples were dispersed in aluminum oxide (5 wt %).

Emission spectra were recorded in a SPEX spectrofluorimeter (Fluorolog 3-22 model), equipped with a double monochromator on both the excitation and emission sides. Emission spectra were registered in suspension using 1 cm quartz cuvettes under 370 nm excitation over a range of 380−650 nm and were corrected for the monochromator and photomultiplier response functions. Excitation and emission slits were 5 and 3 nm, respectively.

Absolute photolunimiscence quantum yields were determined in an integrating sphere (Hamamatsu, model C9920-02) after excitation at 370 nm.

Radiative deactivation curves were recorded by means of the time-correlated single-photon-counting technique (Edinburgh Instruments, model FL 920) with a time resolution of 30 ps after deconvolution of the excitation pulse. The excitation was carried out with diode lasers (PicoQuant, models LDH 370 and LDH 440) at 370 and 440 nm, with pulses of 150 ps fwhm (full width at half-maximum), a repetition rate of 2500 kHz, and a power range between 0.01 and 0.07 mW. The erratic scattering signal of the laser was avoided in the detection channel by filtering the excitation light with 390 and 455 nm cutoff filters, respectively. Two different analyses can be performed of the recorded data from the recorded fluorescent decay curves:

In the lifetime analysis, fluorescence decay curves were measured with 10 000 counts as the maximum for different emission wavelengths: 450, 470, 500, 530, 560, and 590 nm. The FAST software was used for the global analysis; this software allows the simultaneous analysis of the set of multiexponential decay curves recorded at the different excitation and emission wavelengths:

$$I_{fl}(t) = A_1 \exp(-t/\tau_1) + A_2 \exp(-t/\tau_2) + \ldots$$

where A_i represent the pre-exponential factors associated with the statistical weights of each exponential and τ_i are the lifetimes of each exponential decay. The software links the lifetime values τ_i and varies their statistical weights A_i in the fitting of decay curves recorded at the different excitation and

dx.doi.org/10.1021/jp309784y | J. Phys. Chem. C 2012, 116, 26084−26090

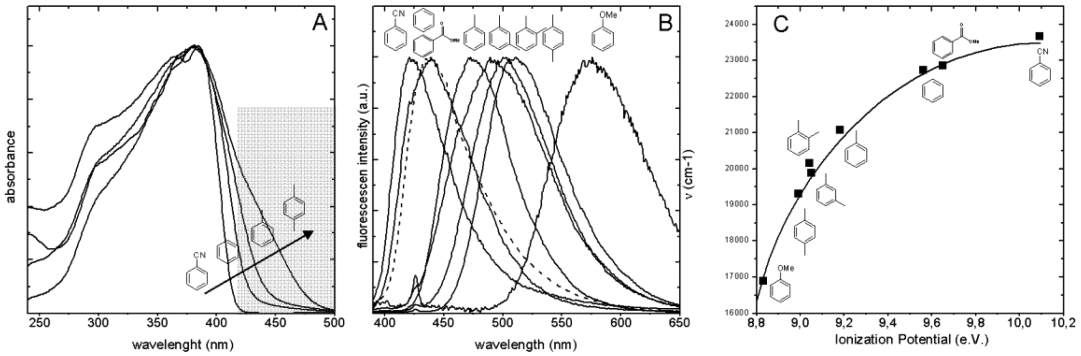

Figure 1. (A) Height-normalized UV−vis spectra by reflectance. (B) Height-normalized fluorescence spectra after excitation at 370 nm. (C) Relationship between the emission maximum (cm^{-1}) and the ionization potential (eV) of PCP with different aromatic guests.

Table 1. Ionization Potentials (IPs, eV), Dipole Moments (μ, D), Quantum Yields (Φ_{fl}), Emission Maxima (λ_{em}, nm), and Lifetimes (τ_i, ns) with Their Respective Statistical Weights (Contribution, %) at Different Excitation (370 and 440 nm) and Emission (≤500 and >500 nm) Wavelengths

						contribution, %		
						370[1] nm excitation wavelength		440[1] nm excitation wavelength
guest	IP	μ	Φ_{fl}	λ_{em}	τ_i	≤500[2] nm emission wavelength	>500[2] nm emission wavelength	>500[2] nm emission wavelength
benzonitrile	10.1	4.6		425	0.1	85	–	–
					0.4	15	–	–
methyl benzoate	9.65	5.2	0.07	440	0.8	75	53	–
					3.0	25	37	–
					17.5	–	10	–
benzene	9.56	0	0.05	440	0.7	32	6	–
					3.2	55	60	–
					7.8	10	26	–
					19.5	3	8	–
toluene	9.18	0.36	0.22	476	0.3	15	8	10
					3.9	15	12	15
					14.0	53	55	45
					17.5	20	25	35
o-xylene	9.04	0.62	0.05	503	0.4	30	10	15
					2.9	50	50	50
					8.9	15	25	15
					25.6	5	15	20
m-xylene	9.05	0.42	0.09	496	0.3	38	13	17
					3.6	25	27	20
					12.6	26	30	22
					23.3	12	30	41
p-xylene	8.99	0.08	0.09	515	0.4	20	5	10
					4.1	25	15	15
					17.1	26	35	25
					27.5	30	45	50
anisole	8.82	1.5	0.01	594	0.4	–	2	2
					3.6	–	48	38
					6.6	–	50	60

emission wavelengths. The results can be easily evaluated using global χ^2 values and local residuals.

For time-resolved emission spectroscopy (TRES), the fluorescence decay curves were recorded as a function of the emission wavelength in the 400−580 nm range (the wavelength increment was 2 nm) for a fixed recording time (300 s per wavelength). The emission spectra at different times after excitation were obtained by averaging the integrated fluorescence intensity for different time windows at every wavelength after the excitation pulse.

RESULTS AND DISCUSSION

To analyze the fluorescence properties, several benzene derivatives with different substituents, from strongly electron-withdrawing to strongly electron-donating capacities, were incorporated as guest aromatic molecules into the pores of $[Zn_2(bdc)_2(NDI)]_n$, such as benzonitrile, methyl benzoate, benzene, toluene, *o*-, *m*-, and *p*-xylene, anisole, and *N*,*N*-dimethylaniline. Other nonaromatic guests such as DMF, cyclohexane, and acetonitrile were used as nonaromatic guest references.

dx.doi.org/10.1021/jp309784y | J. Phys. Chem. C 2012, 116, 26084−26090

Steady-State Absorption and Fluorescence Spectroscopy. Figure 1A illustrates the new absorption shoulder generated in the lower energy region (at 430−470 nm) with respect to the main absorption band of NDI ($\lambda_{ab} \approx 380$ nm). This new shoulder is attributed to the CT complex between the NDI moiety (acceptor or A) and the aromatic guest molecule (donor or D) in the ground state. A confinement effect is noteworthy in this PCP; previous studies in solution[12] concluded that complexation constants between NDI derivatives and aromatic molecules were not large enough to generate charge transfer absorption bands. On the other hand, peak-height-normalized emission spectra (Figure 1B) show a broad fluorescent band that gradually shifts to lower energies with an increase of the electron-donating capacity of the guest molecules, confirming the ionic nature of the emitting species. Thus, with a simple change of the substituent on the phenyl ring, the whole range of the visible spectrum (400−700 nm) is covered, i.e., from 440 nm for benzene (blue) to 475 nm for toluene (cyan), 520 nm for *p*-xylene (green), and 600 nm for anisole (yellow-orange), as shown in Figure 1B. Similar emission bands have been reported for NDI complexes in benzene, toluene, and *p*-xylene solutions, but with significantly lower quantum yields; i.e., for toluene $\Phi_{fl} = 0.22$ in the PCP vs $\Phi_{fl} \approx 0.02$ in solution.[11,12] However, the emission maxima do not linearly correlate with their ionization potentials (Figure 1C). This could indicate not only that the emission is due to a mere charge transfer in NDI−aromatic guest complexes but also that other species/mechanisms could be responsible for the fluorescence.

Fluorescence Time-Resolved Spectroscopy: Lifetime Analysis. To obtain additional information on the emissive species and the photophysical processes involved, we applied time-resolved fluorescent techniques.

Radiative deactivation curves were recorded at different emission and excitation wavelengths for all samples to study their effect on the kinetics of the excited states. Thus, decay curves at two excitation wavelengths were selected: the local excitation of NDI itself at 370 nm (eq 2) and the direct excitation of the CT complex absorption band at 440 nm (eq 1). The registration emission wavelengths were chosen in the range between ≤500 and >500 nm.

Noting that these systems showed a complex dynamics in the excited state, because even decay curves registered in PCP with nonaromatic guests such as DMF, acetonitrile, and cyclohexane, systems with a very poor emission centered at around 425 nm ($\Phi_{fl} < 0.01$) need a biexponential function to be fit (Table S1, Supporting Information). In these samples the very short lifetime, τ_A ≤100 ps (20%), could be attributed to the high scattering of PCP crystals in suspension and/or even an excess of NDI molecules in the solution (characterized by lifetimes of a few picoseconds). A slightly longer τ_B (~350 ps (80%)) was assigned to the structural NDI, being part of the PCP framework because of the increase in the molecular rigidity.

The photophysical properties of PCP with benzonitrile as a guest molecule (Table 1) are very similar to those described above for nonaromatic molecules. The substitution of the cyano group on the phenyl ring does not provide sufficient electron-donating capability to form a CT complex with the acceptor NDI moiety. In fact, benzonitrile does not trigger the structural transformation (framework displacement), and PCP keeps the same structural features as DMF when acting as a guest (Figures S1 and S2, Supporting Information).[11]

Fluorescence decay curves for most of the aromatic guests were analyzed with four decay components (Table 1). To study the effect of emission and/or excitation wavelengths, global decay analysis was performed

Interestingly, the two shorter lifetimes $\tau_1 \approx 0.4$ ns and $\tau_2 \approx 3.5$ ns (Table 1) are common for all the samples independently of the aromatic guests. Therefore, both lifetimes should be attributed to the emission of the species in the framework itself. Regarding the lifetime values previously assigned for non-aromatic guests, the shortest τ_1 is ascribed to the deactivation of structural NDI. Note that, after the accommodation of the aromatic guests, two important structural changes occur in the PCP: the framework displacement and the flattening of structural NDI and the bdc linkers (Figure S2, Supporting Information).[11] Thus, the interaction between the flat bdc and the NDI linkers disposed in contiguous frameworks is now likely fluorescence and is characterized by a lifetime τ_2 of around 3.5 ns. The CT nature of such an "interframework NDI−bdc" interaction can be compared to the one originated between NDI and the substituted benzene guest molecules; however, the fluorescence from the interframework interaction is expected to be very weak because the binding of the carboxylate groups of the bdc molecules to the zinc ion considerably reduces its electron-donating capacity.

Alternatively, lifetimes with longer values, τ_3 and τ_4, strongly vary depending on the nature of the aromatic guests (Table 1). Interactions between the NDI (A) and the aromatic guests (D) generate two lifetimes, τ_3 and τ_4. This fact is attributed to the existence of two different adsorption sites provided by the PCP pores (see Scheme 1, bottom, site A and site B). Thus, aromatic guests lodged at site A are disposed in a more restricted void space and in a parallel configuration with respect to the NDI ligand, whereas guests accommodated in site B are more loose, having a more extended conformation (Scheme 1, bottom). Thus, the relative geometric disposition between the NDI and the aromatic guests in sites A and B would also govern the nature of the complexes and their photophysical properties, i.e., lifetimes.

In general, the excited electronic states of the CT complex and exciplex are a combination between the charge transfer states and exciton resonance contribution of the locally excited states, between its constituents. The wavelength functions can be described as

$$\psi_1^*(\mathrm{CT})^* = C_1\psi(\mathrm{AD})^* + C_2\psi(\mathrm{A^+D^-})^* \quad (3)$$

$$\psi_2^*(\mathrm{EX})^* = C_1\psi(\mathrm{AD})^* + C_2\psi(\mathrm{A^+D^-})^* \quad (4)$$

$$\psi_3^*(\mathrm{CS})^* = \psi(\mathrm{A^{\bullet -}} + \mathrm{D^{\bullet +}}) \quad (5)$$

with CT = charge transfer, EX = exciplex, and CS = charge separation.

Accordingly, face-to-face configurations (π-stacking) between the electron acceptor NDI and the electron donor aromatic guests on site A allow an effective orbital overlapping, providing a higher covalent contribution in the excited state ($C_{2'} > C_2$ in eqs 3 and 4), and are denoted as exciplex $(\mathrm{A-D})^*_{EX}$. On the contrary, the disposition of aromatic guests lodged at site B with respect to the NDI pillar is more open, and thus, the NDI−guest complex would present a more pure ionic character ($C_2 > C_{2'}$ in eqs 3 and 4) and is designated as charge transfer complex $(\mathrm{A^{\delta-}-D^{\delta+}})^*_{CT}$.

Although it is very difficult to independently characterize these two different excited complexes in solution, many authors

dx.doi.org/10.1021/jp309784y | J. Phys. Chem. C 2012, 116, 26084−26090

have claimed their coexistence.[27−33] It is well-known that a slight increase in the solvent's polarity usually causes a drastic reduction of the $(A{-}D)^*_{EX}$ emission due to the promotion to the excited CT state $(A^{\delta-}{-}D^{\delta+})^*_{CT}$, characterized by a lower emission efficiency (most are nonfluorescent in liquid solutions) and a larger red shift than those of the exciplex. According to Barros et al.,[12] the emission of complexes formed by NDI and aromatic compounds (benzene, toluene, and *p*-xylene) was not detectable in polar solvents up to 80% (v/v) aromatic hydrocarbons in acetonitrile, with weak emissions ($\Phi_{fl} \approx 0.002$) centered at around 460, 520, and 560 nm for benzene, toluene, and *p*-xylene, respectively. Fluorescence becomes more intense ($\Phi_{fl} \approx 0.025$) as the aromatic hydrocarbon content increases, shifting to energies of 440, 480, and 520 nm for pure benzene, toluene, and *p*-xylene, respectively, matching perfectly with the maxima described in this work for the PCP system with the same aromatic molecule guests (Table 1).

Generally, discerning the emission of each complex is not an easy task since both species are connected in the excited state. Moreover, fluorescence decay curves are not characterized by a growing-in component, indicative of a very fast excited-state formation for $(A{-}D)^*_{EX}$ and $(A^{\delta-}{-}D^{\delta+})^*_{CT}$ on the femtosecond time scale.[34]

In this particular system, an increase in the contribution of lifetime τ_4 with respect to τ_3 (A_4/A_3) was registered at 440 nm (direct excitation of the ground CT complex $(A^{\delta-}{-}D^{\delta+})_{CT}$) with respect to 370 nm (local excitation of NDI), $(A_4/A_3)_{440} > (A_4/A_3)_{370}$ (Table 1). Thus, τ_3 could be related to the deactivation of the exciplex state $(A{-}D)^*_{EX}$ and τ_4 to the CT complex $(A^{\delta-}{-}D^{\delta+})^*_{CT}$.

Furthermore, it was found that the τ_4 and τ_3 values linearly correlate with the ionization potential ($R = 0.994$) and with the dipole moment ($R = 0.995$) of the guest aromatic molecules (Figure 2), confirming the higher ionic and exciton

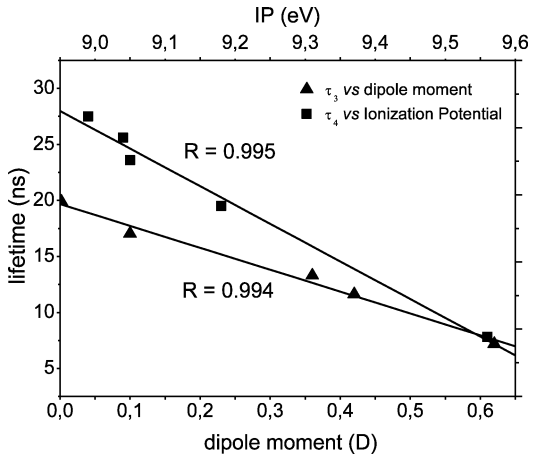

Figure 2. Linear correlation of the exciplex lifetime (τ_3) with the dipole moment and CT complex lifetime (τ_4) with the ionization potential (eV) of the aromatic guests.

contributions for $(A^{\delta-}{-}D^{\delta+})^*_{CT}$ and $(A{-}D)^*_{EX}$ states, respectively. Note that the dipole moment of the guests is considered as the most representative parameter to describe the NDI moiety and aromatic guest interactions. Other common macroscopic parameters related to polarity/polarizability, i.e., dielectric constants, do not make sense here because it has been proved that only one aromatic guest is accommodated per adsorption site,[11] being the guest molecules within PCP pores completely isolated from the surrounding environment as other authors have confirmed.[35] Thus, both pieces of evidence point to τ_3 and τ_4 lifetime values that are related to the deactivation of the exciplex and CT excited states, respectively. The different adsorption sites of PCP allowed the definition of two discrete and distinguishable complexes (exciplex and CT complex) by the different conformations adopted by the aromatic guests with respect to the NDI moiety.

Moreover, and in a similar way to the polarity of the solvent affects the fluorescence of the exciplex and CT complex in solution; in this PCP, the higher the dipole moment and/or the stronger the electron-donating ability of the guest; the more favored the emission from the CT complex over the exciplex (Scheme 2).

Scheme 2. Energy Level Diagram of All the Emissive Species and Processes in PCP[a]

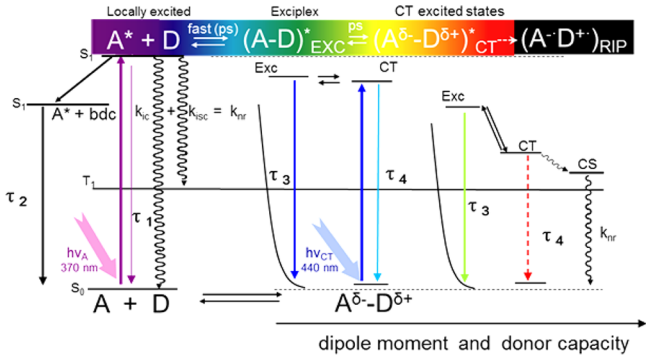

[a]Definitions: τ_1, deactivation of NDI (A); τ_2, deactivation of the interframework complex NDI−bdc (benzenedicarboxilate); τ_3, deactivation of the exciplex NDI−aromatic guest; τ_4, deactivation of the CT complex; LE, locally excited; EXC, exciplex (dissociative in the ground state); CT, charge transfer; CS, charge separation; RIP, radical ion pair.

Note here the clear effect of the dipole for *m*-xylene vs *o*-xylene, both aromatic guests with similar ionization potentials but different dipole moments (Table 1). The steady-state emission band for PCP with *o*-xylene as a guest is slightly red-shifted ($\lambda_{em} = 503$ nm) with less fluorescence ($\Phi_{fl} = 0.05$) with respect to *m*-xylene ($\lambda_{em} = 496$ nm and $\Phi_{fl} = 0.09$) due to the higher dipole moment ($\mu = 0.624$ D vs $\mu = 0.424$ D) that promoted the CT complex over the exciplex state.

PCP with strong electron-donating guests can endorse the total electron transfer process, and fluorescence will be quenched by the conversion to radical−ion pair $(A^{\bullet-}D^{\bullet+})_{RIP}$ states (Scheme 2).

Accordingly, PCP with an anisole molecule, a guest with a relatively high dipole moment and strong electron-donating ability, showed a much reduced quantum yield, $\Phi_{fl} \approx 0.01$, and the long lifetime value of 6.6 ns is much shorter than τ_4 attributed to $(A^{\delta-}{-}D^{\delta+})^*_{CT}$ states, denoting a partial deactivation process to the $(A^{\bullet-}D^{\bullet+})_{RIP}$ state (Scheme 2). Note that this guest only provides triexponential decay curves (Table 1) and does not trigger the structural transformation, keeping the DMF-type structure (Figure S1, Supporting Information), likely due to the high promotion to the CT excited state, and the exciplex emission becomes negligible.

PCP with the strongest donating guest, *N*,*N*-dimethylaniline, showed a deep purple color with a characteristic absorption band at 550 nm (Figure 3A) and a totally quenched

dx.doi.org/10.1021/jp309784y | J. Phys. Chem. C 2012, 116, 26084−26090

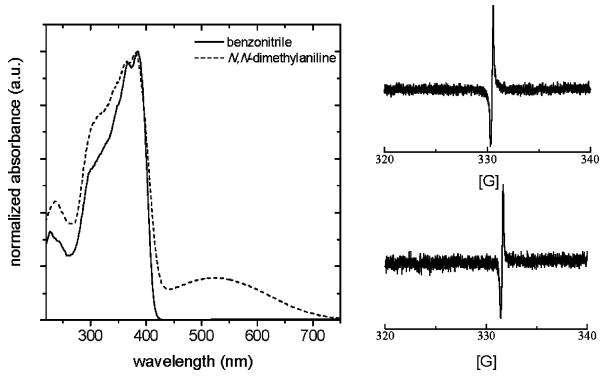

Figure 3. (A, left) Height-normalized absorption spectra of benzonitrile (solid line) and *N*,*N*-dimethylaniline (dashed line). (B, right) ESR signal of PCP with *N*,*N*-dimethylaniline as a guest molecule recorded at 77 K and room temperature.

fluorescence, typical for NDI anion radical species.[14] The anion radical stabilization was confirmed by the ESR signal (Figure 3B). Studies on radical anion generation for similar NDI derivate compounds in solution found they could be yielded with higher than 70% conversion but could be retained for up to 2 h after the reduction experiments.[14] In this PCP, stabilization of NDI anion radical species was achieved over long periods of time (several days, even months).

In summary, Scheme 2 illustrates the effect of the dipole moment and the electron-donating capacity of the guests on the energy diagram of the excited electronic states of PCP with NDI as a photoactive moiety. Generally, an increase of the dipole moment and/or the electron-donating capacity of the aromatic guest molecules gradually stabilizes the excited CT complex over the exciplex state, and consequently, the emission band progressively shifts to the red, reducing the fluorescence efficiency until it is totally quenched by the formation of the radical ion species.

Time-Resolved Emission Spectra. Although steady-state fluorescence spectra showed only a broad band for all the guests, time-resolved emission spectra could resolve the overlapped emission bands of the emissive species by their different lifetime values. Figure 4 shows the time-resolved emission spectra of three representative samples: benzene (A), methyl benzoate (B), and *o*-xylene (C).

At short times after the laser pulse, $t \leq 3$ ns, all samples show a fluorescence band centered at around 430−440 nm (Figure 4, spectra a and b), identified as interframework NDI−bdc complexes, characterized by a lifetime τ_2 of around 3−4 ns. However, for longer times after the pulse (>6 ns), the evolution of the emission bands is very different depending on the aromatic guest molecules, as lifetimes τ_3 and τ_4 have already been assigned to NDI−aromatic guest interactions.

Thus, in the first example (Figure 4A), for *o*-xylene as the guest, as the time after the pulse increases, it is possible to see the evolution from the bdc−NDI interframework CT emission at short lifetimes (spectra a and b) at 440 nm to the NDI−guest exciplex band placed at around 485 nm (spectra c and d) and the red-shifted CT complex emission (at 503 nm) at long times after the pulse (spectra e and f).

Other interesting evolution in the time-resolved emission spectra is observed in Figure 4B,C for benzene vs methyl benzoate guest molecules with similar steady-state fluorescence spectra (Figure 1B, solid line (benzene) and dashed line (methyl benzoate)), but quite different emission bands at long times after the laser pulse. Although both aromatic molecules have similar electron-donating abilities, methyl benzoate is characterized by a much higher dipole moment than benzene (Table 1). Thus, due to the greatly stabilized CT excited state, $(A^{\delta-}-D^{\delta+})^*_{CT}$, the methyl benzoate guest shows a very red-shifted emission band, placed at around 510 nm, with respect to benzene guest molecules, at around 450 nm, for long times after the laser pulse (Figure 4B,C, spectra d−f). Note that, similar to the case of anisole, PCP with methyl benzoate guest molecules keeps the DMF-type structure and also provides triexponential decay curves. Indeed, in Figure 4C there is not any evidence of intermediate bands to be ascribed to exciplex emission, as has been observed for *o*-xylene (Figure 4A). These experimental results indicate that the structural transformation of PCP is mainly triggered by the exciplex formation between certain aromatic guests and the photoactive pillar NDI, generating in the structure the characteristic slit-type pore (site A) for face-to-face interactions.

CONCLUSIONS

In the present work, emissions from both exciplex and charge transfer complex states are photophysically characterized thanks to the particular construction of this entangled PCP, $[Zn_2(bdc)_2(NDI)]$, with NDI (acceptor) in an ordered 3D sequence and the confinement of different aromatic guests (donors) into the two geometrically defined pores: site A (slitlike pore in which the aromatic guest molecules interact in a

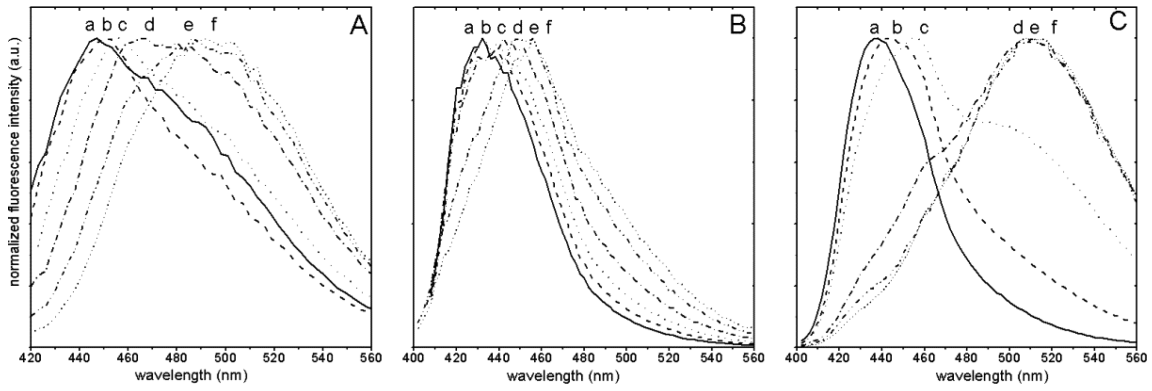

Figure 4. Time-resolved emission spectra at different times after the pulse, (a) 0−0.5 ns, (b) 1−3 ns, (c) 4−6 ns, (d) 8−10 ns, (e) 11−15 ns, and (f) 20−30 ns, for (A) *o*-xylene, (B) benzene, and (C) methyl benzoate as guests.

dx.doi.org/10.1021/jp309784y | J. Phys. Chem. C 2012, 116, 26084−26090

face-to-face manner with the NDI ligand) and site B (undulated one-dimensional channel where aromatic guest molecules are not so structurally restricted).

The fluorescence lifetime of the exciplex linearly correlates with the dipole moment of the guests due to the important resonance contribution (π-orbital overlap) in the excited state, whereas the lifetimes of the CT complexes correlate with the ionization potential of the guests because of the more ionic nature of their excited states. Emissions from charge transfer states are characterized by longer lifetimes and red-shifted and lower efficiency fluorescence bands with respect to exciplex emission and are promoted as the dipole moment and/or electron-donating capacity of the guests increase. In extreme cases, the CT complex endorses the total electron transfer process, and fluorescence will be quenched by the conversion to a radical−ion pair. Other emissive species with much lower emission efficiency were identified: structural NDI and the bdc−NDI intraframework complex characterized by shorter lifetimes of around 0.4 and 3.5 ns with characterized emission in the higher energies region at around 420−440 nm.

As a brief conclusion, using the topological principles of PCP systems (highly crystalline and flexible structure, intrinsic porosity, and designability to accommodate chromophores in a 3D order), they can be considered as a model for the investigation of many photophysical phenomena.

■ ASSOCIATED CONTENT

Supporting Information

X-ray powder diffraction patterns, X-ray crystallographic information, TG data, and photophysical parameters. This material is available free of charge via the Internet at http://pubs.acs.org.

■ AUTHOR INFORMATION

Corresponding Author

*E-mail: virginia.martinez@ehu.es.

Notes

The authors declare no competing financial interest.

■ ACKNOWLEDGMENTS

We are thankful for the financial support of the Industry Program from the Basque Government, Saiotek project (S-PE10UN65, S-PE11UN64 and S-PE12UN140). V.M.M. acknowledges Gobierno Vasco IT339-10 (<2012) and the Ramón y Cajal program from the Ministerio de Economía y Competitividad (>2012) for a research contract. iCeMS is supported by the World Premier International Research Initiative (WPI), MEXT, Japan.

■ REFERENCES

(1) Yaghi, O. M.; O'Keeffe, M.; Ockwing, N. W.; Chae, H. K.; Eddaoudi, M.; Kim, J. *Nature* **2003**, *423*, 705−714.

(2) Kitagawa, S.; Kitaura, R.; Noro, S. *Angew. Chem., Int. Ed.* **2004**, *43*, 2334−2375.

(3) Ferey, G. *Chem. Soc. Rev.* **2008**, *37*, 191−214.

(4) Farha, O. K.; Hupp, J. T. *Acc. Chem. Res.* **2010**, *43*, 1166−1175.

(5) Sumida, K.; Rogow, D. L.; Mason, J. A.; McDonald, T. M.; Bloch, E. D.; Herm, Z. R.; Bae, T. H.; Long, J. R. *Chem. Rev.* **2012**, *112*, 724−781.

(6) Li, J. R.; Sculley, J.; Zhou, H. C. *Chem. Rev.* **2012**, *112*, 869−932.

(7) Corma, A.; Garcia, H.; Llabré i Xamena, F. X. *Chem. Rev.* **2010**, *110*, 4606−4655.

(8) Kreno, L. E.; Leong, K.; Farha, O. K.; Allendorf, M.; Van Duyne, R. P.; Hupp, J. T. *Chem. Rev.* **2012**, *112*, 1105−1125.

(9) Allendorf, M. D.; Bauer, C. A.; Bhakta, R. K.; Houk, R. J. T. *Chem. Soc. Rev.* **2009**, *38*, 1330−1352.

(10) Yuanjing, C.; Yanfeng, Y.; Guodong, Q.; Banglin, C. *Chem. Rev.* **2012**, *112*, 1126−1162.

(11) Takashima, Y.; Martínez-Martínez, V.; Furukawa, S.; Kondo, M.; Shimomura, S.; Uehara, H.; Nakahama, M.; Sugimoto, K.; Kitagawa, S. *Nat. Commun.* **2011**, *2*, 168.

(12) Barros, T. C.; Brochsztain, S.; Toscano, V. G.; Berci Filho, P.; Politi., M. J. *J. Photochem. Photobiol., A* **1997**, *111*, 97−104.

(13) Cho, D. W.; Fujitsuka, M.; Yoon, U. C.; Majima, T. *J. Photochem. Photobiol., A* **2007**, *190*, 101−109.

(14) Andric, G.; Boas, J. F.; Bond, A. M.; Fallon, G. D.; Ghiggino, K. P.; Hogan, C. F.; Hutchison, J. A.; Lee, M. A. P.; Langford, S.; Pilbrow, J. R.; Troup, G. J.; Woodward, C. P. *Aust. J. Chem.* **2004**, *57*, 1011−1019.

(15) Viehbeck, A.; Goldberg, M. J.; Kovac, C. A. *J. Electrochem. Soc.* **1990**, *137*, 1460−1466.

(16) Ilmet, I.; Berger, S. A. *J. Phys. Chem.* **1967**, *71*, 1534−1536.

(17) Alp, S.; Erten, S.; Karapire, C.; Köz, B.; Doroshenko, A. O.; Icli, S. *J. Photochem. Photobiol., A* **2000**, *190*, 103−110.

(18) Parker, C. A. *Photoluminiscence of Solutions*; Elsevier: Amsterdam, 1968.

(19) Birks, J. B. *Photophysics of Aromatic Molecules*; Wiley-Interscience: London, 1970.

(20) Kawakami, J.; Nakamura, J.; Iwamura, M. *J. Photochem. Photobiol., A* **2001**, *140*, 199−206.

(21) Lauteslager, X. Y.; van Stokkum, I. H. M.; van Ramesdonk, H. J.; Bebelaar, D.; Fraanje, J.; Goubitz, K.; Schenk, H.; Brouwer, A. M.; Verhoeven, J. W. *Eur. J. Org. Chem.* **2001**, *16*, 3105−3118.

(22) Jiang, H.; Xu, H. *J. Chem. Soc., Perkin Trans.* **2001**, *2*, 1274−1279.

(23) Knibbe, H.; Rolling, K.; Schafer, F. P.; Weller, A. J. *Phys. Chem.* **1967**, *47*, 1184−1185.

(24) N. Mataga, T.; Okada, H.; Masuhara, N.; Nakashima, Y.; Sakata, S.; Misumi, J. *Luminiscence* **1976**, *12/13*, 159−168.

(25) Prochorow, J. *J. Mol. Struct.* **1997**, *404*, 199−211.

(26) Cho, D. W.; Fujitsuka, M.; Sugimoto, A.; Yoon, U. C.; Mariano, P. S.; Majima, T. *J. Phys. Chem. B* **2006**, *110*, 11062−11068.

(27) Schryver, F. C.; Boens, N.; Put, J. *Adv. Photochem.* **1977**, *10*, 359−465.

(28) Verhoeven, J. W.; Scherer, T.; Willemse, R. J. *Pure Appl. Chem.* **1993**, *65*, 1717−1722.

(29) Scherer, T.; Van Stokkun, I. H. M.; Brouwer, A. M.; Verhoeven, J. W. *J. Phys. Chem.* **1994**, *98*, 10539−10549.

(30) Grabowsli, Z. R.; Roetkiewicz, K. *Chem. Rev.* **2003**, *103*, 3899−4031.

(31) Rath, M. C.; Pal, H.; Mukherjee, T. *J. Phys. Chem. A* **1999**, *103*, 4993−5002.

(32) Kwan, P. H.; Swager, T. M. *J. Am. Chem. Soc.* **2005**, *127*, 5902−5909.

(33) Saito, H.; Mori, T.; Wada, T.; Ionue, Y. *J. Am. Chem. Soc.* **2004**, *126*, 153−157.

(34) Ganesan, P.; Baggerman, J.; Zhang, H.; Sudhölter, E. J. R; Zuilhof, H. *J. Phys. Chem. A* **2007**, *111*, 6151−6156.

(35) Choi, J. R.; Tachikawa, T.; Fujitsuka, M.; Majima, T. *J. Phys. Chem. Lett.* **2010**, *1*, 1101−1106.